

# Chapter 4

## Fast Gas Chromatography: Design, construction and evaluation of a fast gas chromatograph

### 4.1 Introduction

In this chapter the design and construction of a gas chromatograph capable of very fast temperature programming rates is described. Computer controlled, fast heating rates were obtained through direct resistive heating of a stainless steel capillary column. The current through a conductive metal capillary was controlled through feedback to follow a set temperature ramp with fidelity. A user-friendly PC based interface was designed.

Various temperature measurement circuits were built and compared for ease of implementation.

The retention time reproducibility of the constructed fast resistively heated GC is compared with that of other resistively heated gas chromatographs, as reported in the literature.

The linear gas flow and temperature-programming rates were optimized following the recommendations made by Blumberg<sup>1</sup>. This optimized fast resistively heated GC was used for construction of the comprehensive SFCxGC<sub>ftp</sub>.

### 4.2 Instrumentation

#### 4.2.1 Column and electrical connections

A Varian 3300 GC (Varian Inc., MA, USA) was used to host the fast resistive GC. Mainly the gas plumbing and detectors of the host GC were needed, however the oven

---

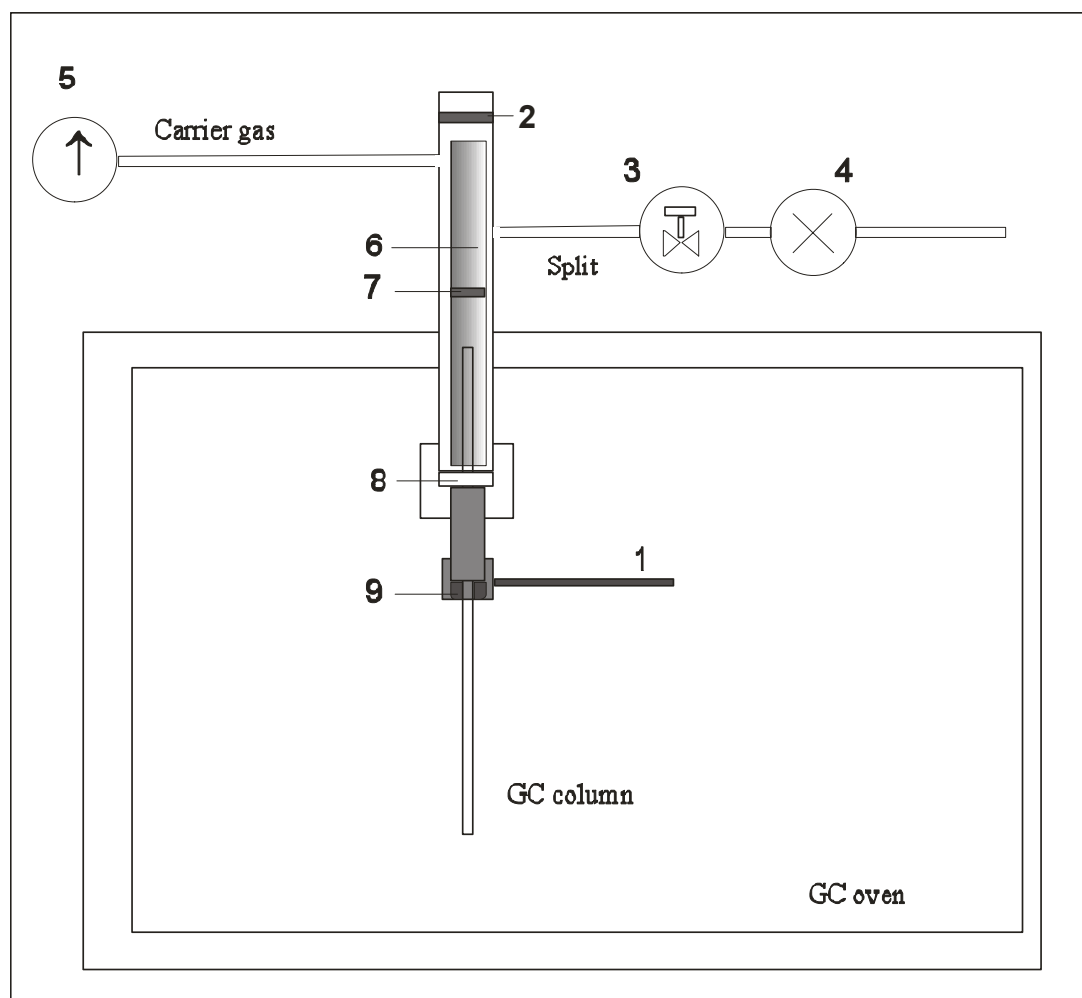
<sup>1</sup> L.M.Blumberg, M.S.Klee, J.Microcol.Sep. 12 (2000) p508

was useful for maintaining a stable, temperature controlled environment. The cryogenic facility was convenient for cooling down the column after analysis. The temperature control printed circuit board on the Varian was modified to allow remote and independent command over the oven heater, oven fan and cryogenic cooling facility by the controlling computer. This was done by respectively forcing pin 1 on U22, U23 and U26 to TTL low. R47 was also forced to TTL low to deactivate the 'Fault 21'-message indicative of a problem with the heating circuitry<sup>2</sup>.

**Figure 4-1: Schematic diagram of injector connections.**

**Detector connections are similar.**

- |                               |   |
|-------------------------------|---|
| 1.Connection to power supply, | 2.Septum,                                     |
| 3. Needle valve               | 4.Computer actuated solenoid valve,           |
| 5.Pressure control            | 6.Glass insert,                               |
| 7.Frit ,                      | 8.Insulation(ceramic disk and vespel ferrule) |
| 9.Graphite ferrule.           |   |



<sup>2</sup> R.Strydom, Personal communication, SMM Instruments, SMM House, Kyalami Business Park, Midrand, 1685, South Africa

---

A one-meter section of 0.25mm i.d. SE-30 stainless steel column (Quadrex Corp. SS Ultra alloy) was tightly coiled. After release, the coil diameter relaxed to 1.5cm. The column was connected to the split/splitless injector and FID detector on the host GC. A 30V-power supply was connected to the heated column connectors on the injector and detector legs. Electrical connections were made by silver soldering thick copper leads to the column connection screws. Graphite ferrules ensured good electrical contact between the connectors and the metal column. The detector and injector legs were electrically insulated from the body of the GC by using pure Vespel ferrules between the injector and detector legs and their bodies. At the detector side, the intruding section of the leg was painted with poly-imide resin to prevent electrical contact higher-up inside the detector body. On the injector side a ceramic washer was placed between the spring, that keeps the injector liner in place, and the injector column connector, that protrudes into the oven.

All electrical connections between the electronics-box, column and PC were through a SCB-68 connector block accessory (National Instruments, Texas,USA).

#### ***4.2.2 Current Control***

The current delivered by a DC power supply (King Electronics Company, (Pty) Ltd ) was controlled by changing the value of a 0-5V DC-out signal derived from a multipurpose data acquisition (DAQ) board (PCI-6024E, National Instruments).

The control output was amplified with an operational amplifier (LM 741). The output from the operation amplifier was connected to the base of a power transistor (Details given below). By changing the bias to the base of the power transistor, the current output of the supply through the column was controlled. While the power supply can deliver 6A, typically less than 3A was required to heat the 1 meter resistive column at all practical rates.

Two different current control circuits were used depending on the method of temperature sensing:

For the Resistive Measurement Circuit (Figure 4-4) the column was connected to the collector of a PNP power transistor. The base of the power transistor was connected to the collector of a smaller NPN transistor. In this way enough current could be supplied to drive the larger power transistor.

---

For the AC measuring circuits the power transistors (3 Darlington pairs used in parallel) were connected between the column and ground potential as opposed to between the power supply and the column. A Darlington pair is similar to the situation described above where a smaller transistor drives a bigger one. In this case it was convenient to have both transistors in the same package. Three transistors were used in series to prevent self-heating effects. This second power circuit was used for thermocouple measurements but here either circuit could be used.

### ***4.2.3 Temperature sensing***

Five different methods of temperature sensing were attempted.

#### ***4.2.3.1 Philips circuit***

A circuit based on the one described by Philips<sup>3</sup> was constructed. A 10kHz square wave pulse train was created from a counter chip on the DAQ board. LabVIEW Program 1.a <*simple control.vi*> was used. This was connected through an optically coupled switch (NTE3085), operated in conjunction with an 8V isolated power supply to protect the computer from the high voltage and current present on the column during programming. The 10kHz signal was applied across the column and coupled in a capacitive manner to a voltage following amplifier. The output from the amplifier was connected to an analog input on the DAQ where it was sampled at 20kHz. Sampling was synchronized to wave generation by using LabVIEW's built-in *triggered acquisition.vi*. This ensured that the samples were taken from the center of each pulse. Sample averaging was used to compensate for noise and thus improve accuracy of measurements.

The height of each digital conversion is related linearly to the electrical resistance of the column and thus to the temperature through Equation 3-18. Calibration of the system was achieved through measuring the height of the pulse train at several known temperatures, obtained from the host GC oven. The LabVIEW *PID.vi*, obtained from the PID control toolkit, was incorporated into the operating program to facilitate temperature feedback control.

---

<sup>3</sup> V.Jain, J.B.Philips, J.Chrom Sci. 33 (1995) p55

Figure 4-2: The Philips circuit

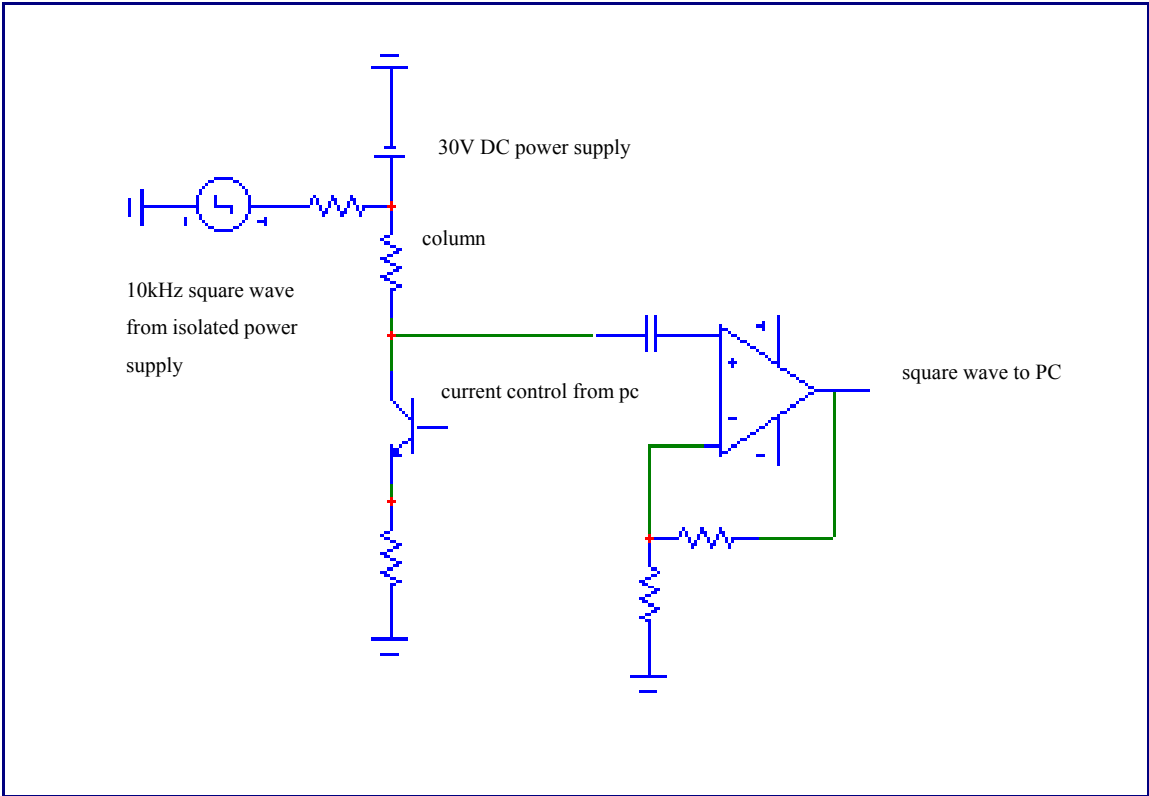
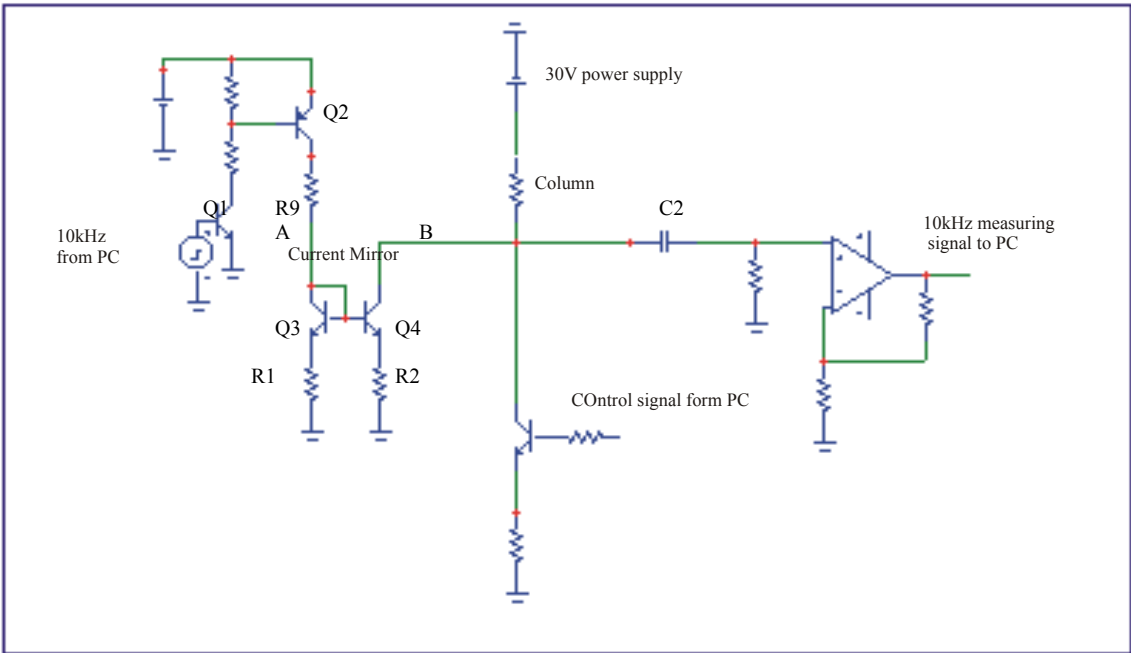


Figure 4-3: The current mirror circuit



#### 4.2.3.2 *Current mirror circuit*

The measuring signal can be coupled through a *current mirror* to the column. The current mirror is a device that ensures that the currents through both collectors of the two transistors are equal. This implies that the current through B (Figure 4-3) and thus through the column, is the same as the current that flows through A. Resistor R1 and R2 are included to improve current stability, which may otherwise vary by 25% due to the Early effect<sup>4</sup>. The current through A is determined by the resistance and the voltage across R9. This was set to 50mA by using an 8V isolated power supply and a 150 $\Omega$  resistor. However the measured current that flowed into the collector of Q3 was only 30mA.

In this way the 5mA square wave from the output of the counter chip was increased to the 30mA by transistor Q2 and Q1 through resistor R9.

The current through Q4 was supplied from the power source that effected heating. This produced a square wave on the column that followed the wave supplied by the counter chip on the computer. The same 10kHz AC pulse train, as used in the previous circuit, was used.

The AC measuring signal was connected to an analog input channel on the DAQ through a high-pass filter. Differential signal connections were used. The same LabVIEW programs (1.a) as used for the Philips circuit were used.

#### 4.2.3.3 *The Resistance Measurement Circuit*

With this circuit the resistance of the column is obtained through measurement of the Voltage drop and the current through the column. This is used as an indication of column temperature. The Voltage drop across the column was measured by reading the potential difference over the column. The voltage difference between points A and B in Figure 4-4 is an indication of the voltage drop due to the resistance of the column. A second voltage drop was measured across a fixed resistor. This reading is proportional to the current through the column as long as the value of this resistor is known and fixed. Five 4.7 $\Omega$ , 25W resistors were connected in parallel to prevent self-

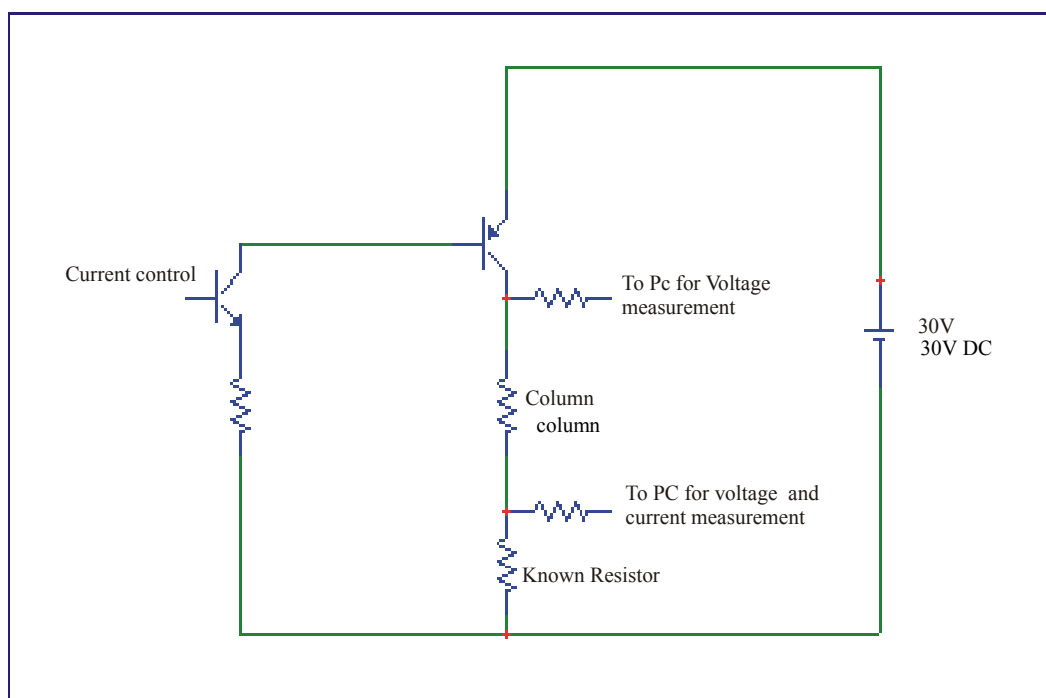
---

<sup>4</sup> P.Horowitz, W.Hill, The art of electronics, 2<sup>nd</sup> ed. (1995) Cambridge University Press p88

heating and keep the temperature of the resistors low and constant. This produced a resistance of  $1\Omega$  with a 125W power rating. The resistors were also mounted on a heat sink. A small current of 100 mA was required when the column was not heated to allow readings to be taken. Signal averaging of input voltages was used to compensate for noise.

(See LabVIEW Programs 2.a and 2.b)

**Figure 4-4:** The resistive circuit



#### 4.2.3.4 Thermocouple Measurements

A very small thermocouple was constructed from type K thermocouple wire (  $T1 = \text{Ni}90/\text{Cr}10$ ;  $T2 = \text{Ni}95/(\text{Al}+\text{Mn}+\text{Si})5$  ). The wires had diameters of 25 micrometer and were insulated with a poly-imide coating (Goodfellow, Cambridge GB). The poly-imide coating was removed from the ends of the two wires with a butane cigarette lighter by holding the them about 3 cm above the flame.

Two methods of making the very small thermocouples were tested:

- The stripped ends of the two wires were twisted. Silver solder was dipped in flux and melted in a butane/air flame. The twisted pair of thermocouple wires

was then pulled through the ball of molten solder. Best results were obtained when the twisted ends were pulled through first with the legs following. This produced a big blob at the outer end that tapered off towards the legs. This could then be trimmed with a scalpel to give a small thermocouple.

While thermocouples could be produced in this way, the procedure had to be repeated many times to yield a satisfactory thermocouple. Much time and expensive thermocouple wire were wasted in the process.

- In contrast, making the thermocouple by spot welding was relatively easy and produced a much smaller thermocouple. A special procedure had to be followed to ensure that the current did flow through the thin thermocouple wires and not directly between the two spot welder-contacts. The following method was used:

A copper base plate was connected to the ground potential of the welder. On the high potential side a sharply pointed probe was connected. The polyimide coating was removed from the ends of the wires. The stripped ends of the thermocouple wires were crossed on an insulating material and were extended onto the grounded base-plate where it was kept in place with sticky tape. Contact was made to the wires just before the cross while ensuring that both wires were in contact with the probe. See Figure 4-5.

**Figure 4-5: Photograph showing how thermocouple wires are positioned for making a thermocouple by spot welding.**



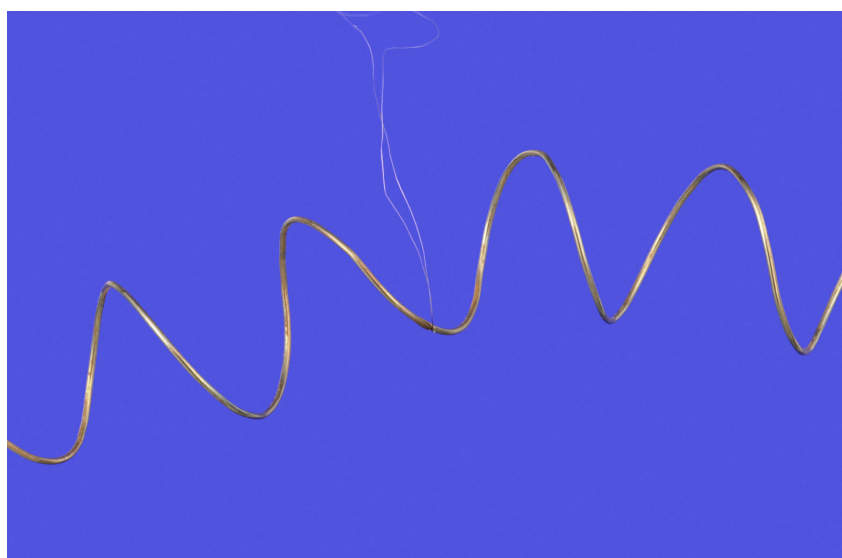


In this way it was ensured that the current flowed through the thermocouple wires to the base plate. When energy was discharged, the two wires melted together at the cross to form a thermocouple. With both methods, the resistance of the thermocouple wires were tested with a multimeter to ensure that the wires are joined properly.

The thermocouple was glued to the column using poly-imide resin (Figure 4-6). A little polyimide resin was painted onto the column. This tended to pull into a droplet on the column. A small heating current was applied to the column to facilitate evaporation of the toluene solvent. After the resin became sticky the thermocouple was submerged into the drop and held in place by hand for a minute or two until set. A larger current was then applied until the temperature reading, as measured on the column, remained constant indicating that all the toluene had evaporated. No thermocouple calibration was required and cold junction compensation was automatically programmatically performed by the LabVIEW drivers (NIDaq version 5.7).

Thermocouples were differentially connected through a 40Hz low band pass RC filter to an analog input on the SCB-68 accessory. Two 100K $\Omega$  bias resistors were connected between each of the wires and ground potential. LabVIEW program 3.a and 3.b were used for control of the resistively heated gas chromatograph.

**Figure 4-6: The thermocouple is glued to the coiled column**



#### ***4.2.3.5 Fixed current ramp***

The thermocouple readings, taken repeatedly at many temperatures, were used to define a current ramp. The output values were recorded and Microsoft Excel was used to obtain the average function. The coefficients had to be adjusted through an iterative process until the required ramp was followed with acceptable fidelity. This was checked by thermocouple readings, measured concurrently with column heating. The ramp was applied to the column without feedback control.

#### ***4.2.4 Data collection***

The A/D converter on the Varian FID board was too slow to be used for fast GC data collection. Instead a fast variable response rate converter was salvaged from an old magnetic sector mass spectrometer (VG model FA3). The output from the FID was connected directly to the preamplifier of the FA3. The signal was collected by Chromperfect Software (Justice Innovations) after amplification.

#### ***4.2.5 Reproducibility***

The reproducibility of the fixed current ramp and the thermocouple were investigated and compared with the published reproducibility results of other resistive GC's. Unfortunately, the others circuits could not be persuaded to yield temperature programs and were not tested for reproducibility. 0.2 $\mu$ L of a sample containing n-alkanes between decane and tetracosane in CS<sub>2</sub> was injected by hand 10 times.

#### ***4.2.6 Optimization of rate***

Following the work by Blumberg, the adequate separation of a required number of analytes in the shortest time was found by increasing the flow rate and temperature programming rate, while keeping the normalized ramp rate constant. A sample containing the n-alkanes between C<sub>10</sub> to C<sub>24</sub> was made up in CS<sub>2</sub> and injected at each set of ramp and flow rates. The peak capacity obtained was calculated and plotted against analysis time. Each set was repeated three times.

## 4.3 Results and discussion

### 4.3.1 General comments

Commercial stainless steel columns did not produce the problems encountered due to differences in expansion coefficients experienced with aluminum clad or painted columns, more over they appeared to be stable and unreactive. The manufacturers claim that the walls are very homogenous in diameter and thickness<sup>5</sup>. This ensured constant heating across the length of the capillary. With a resistance of  $\approx 11\Omega/\text{m}$  there was no need for coating the capillary with an additional conductive layer. The resistivity of UltraAlloy was found to be  $162\mu\Omega/\text{m}$ . The larger the temperature coefficient (tempco), the larger the increase in output for a given increase in temperature. Higher tempcos mean that temperature set points can be followed with more accuracy. While less sensitive than aluminum and Nickel, the tempco of UltraAlloy compares favorably with other metals of high resistivity. This makes Ultra Alloy a good material for the measurement of temperature as a function of resistance.

**Table 4-2: Resistance data of common metals<sup>6</sup>**

Material	Resistivity ( $\mu\Omega.\text{cm}$ )	Temperature coefficient of resistance ( $\Omega/\Omega/^\circ\text{C}$ )
Nichrome	108	0.00036
304 SS	73	0.00094
321 SS	71	0.00123
Nickel	8	0.006
Aluminium	2.67	0.00446
UltraAlloy*	162	0.00099

\*Experimentally determined

The column can be tightly coiled. A diameter less than 1 cm can be tolerated without loss of deactivation<sup>5</sup>. Upon release of tension, the coil maintains its structure and no additional support was required to keep it in shape or to insulate individual turns. The

<sup>5</sup> [http://www.frontier-lab.com/products/column/Ultra\\_ALLOY\\_Columns.html](http://www.frontier-lab.com/products/column/Ultra_ALLOY_Columns.html)

<sup>6</sup> R.S.Scharlach, Electronic Design, 22, (1979) p106

advantage to this is a reduced thermal mass, which translates into faster heating and cooling rates.

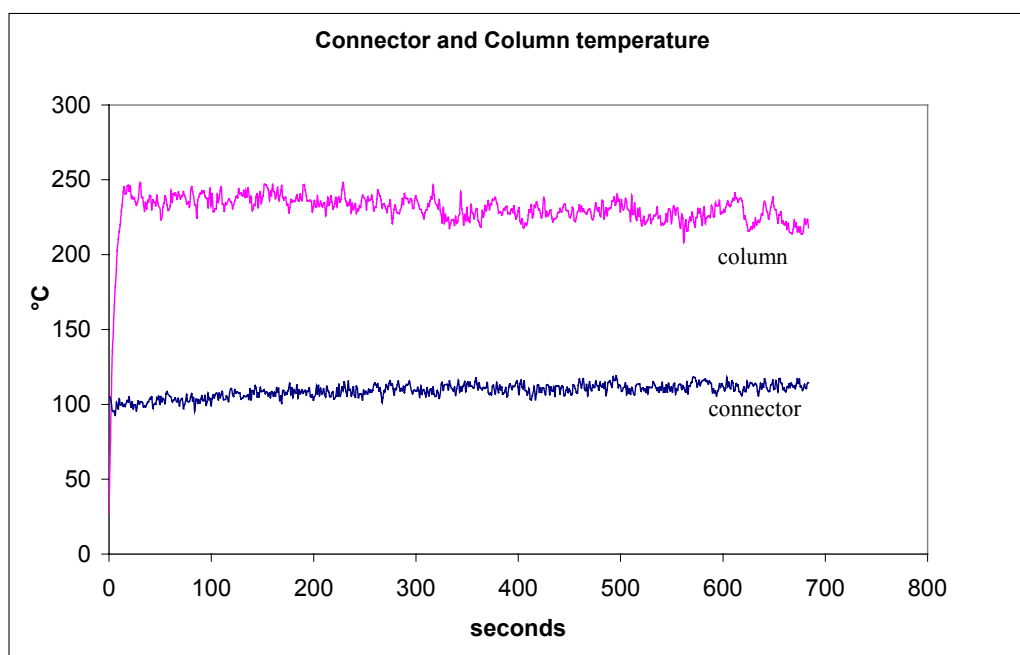
While using the commercial column without additional heating-sleeves provided flexibility in column length, in practice the column length was limited to 1 meter by the size of the oven. It was impossible to use longer columns without the column touching the sides of the oven, causing a short-circuit to ground potential. A longer column would increase plate numbers. This would be beneficial for the separation of the complex fractions transferred from the SFC.

One disadvantage of heating the SS-column directly is that currently they are only available in a few inner diameters. The narrowest column available has an inner diameter of 0.25 mm. A narrower bore would be advantageous for increasing plate number production per unit time for fast chromatography.

#### 4.3.2 Additional heating of injector and detector legs

##### Figure 4-6: Temperature of injector and detector legs during a temperature ramp.

Detector and injector temperatures were set to 280°C. Resistively heated column at 250°C. Host GC oven at 40°C.



---

The column was installed into the column connectors (legs) of the injector and detector on the host GC. These were heated up to 280°C to ensure that the electrical connections did not cause cold spots at the point of connection. The responses of the different circuits were then calibrated by increasing the oven temperature. However, it was soon realized that the results obtained with the resistively heated GC did not match those made under similar conditions where the temperature was controlled by the host GC oven. With the resistively heated GC, the peaks produced by less volatile compounds would take longer to elute than expected and severe tailing was observed. After investigation it was found that the mounted block heaters did not heat the injector and detector legs adequately. While the injector and detector bodies were at 280°C, temperatures below 100°C were measured on the legs protruding into the GC oven (Figure 4-6). With conventional use of the Varian GC it is never a problem, as the protruding column connectors are heated up with the oven temperature as it is programmed. To circumvent this problem, additional heaters were installed around the column connectors to ensure proper heating. This was achieved by connecting a VariAC to an insulated heating tape and winding the heating tape around the injector and detector column connectors. The temperature was measured with a thermocouple and the voltage was manually regulated to maintain the temperature at or above the maximum of the column ramp.

After this, the shape and elution pattern of the chromatogram obtained with the resistively heated GC more closely resembled the chromatograms obtained with the conventional temperature programmed GC.

The four different temperature-sensing circuits, discussed in the previous section, were built for comparison. However, only the thermocouple, thus far, produced usable results. The various circuits and their problems are discussed below.

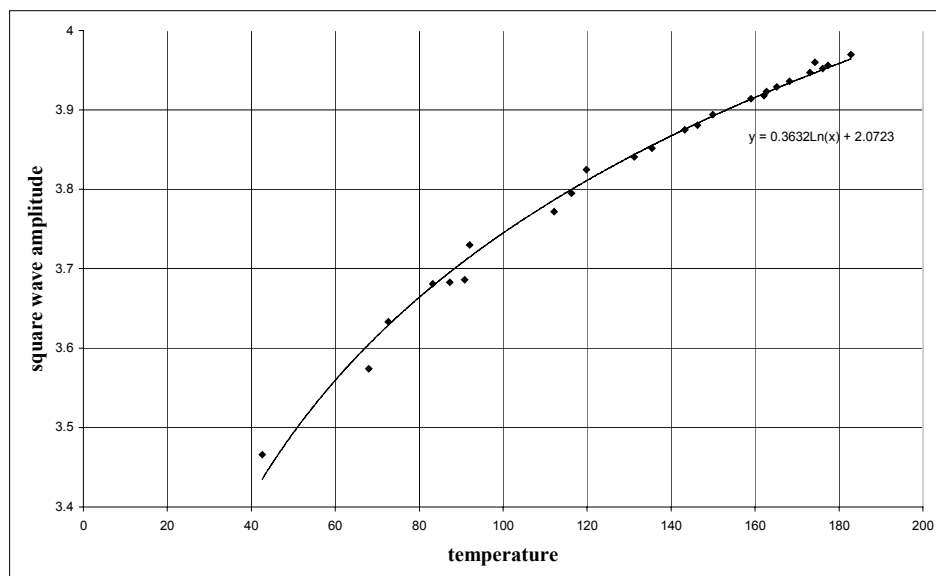
### ***4.3.3 The Philips circuit***

The use of a square wave for measurement has two advantages:

1. The measurement-current flows only half the time and probability of noticeable heating of the column by the sensing current is reduced.
2. The AC measurement signal can be extracted from the DC heating current and from environmental electronic noise.

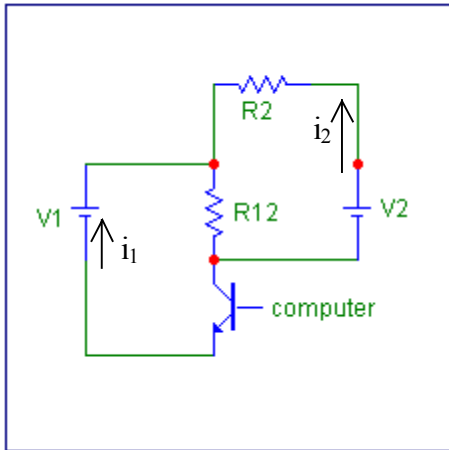
The heating current control can only be seen as a perfect current source if the power transistor remains at a constant temperature. Three TIP-142's were used in parallel and mounted to a heat sink with fan to ensure isothermal operation.

**Figure 4-7: Calibration curve obtained for Philips circuit**



By placing the column in the oven and obtaining amplitude readings at known temperatures, maintained by the host GC, an exponential temperature versus amplitude calibration curve could be obtained. The measured amplitude of the square wave increased with  $\approx 1.5$  volts across the  $300^{\circ}\text{C}$ -temperature range. This correlates to a  $5\text{mV}$  increase per  $^{\circ}\text{C}$ . With the 12bit AD converter used, a resolution of  $0.01^{\circ}\text{C}$  could potentially be obtained.

However, when a heating current was applied erroneous readings were obtained. Readings would decrease when the heating current was switched on to readings much lower even than any of those measured for the calibration curve.

**Figure 4-8: Simplified Philips circuit**

The circuit is based on the assumption that the measuring current  $i_2$  and the heating current  $i_1$  are independent. Applying Kirtchoff's law, which states that the sum of currents into a point in a circuit equals the sum off currents out<sup>7</sup>, revealed a fundamental flaw in this approach:

$$i_1 = const$$

$$v_2 = i_2 R_2 + i_2 R_{12} + i_1 R_{12}$$

$$v_2 - i_1 R_{12} = i_2 (R_2 + R_{12})$$

$$i_2 = \frac{v_2 - i_1 R_{12}}{R_2 + R_{12}}$$

$$v_2 = 8V, R_2 = 300\Omega, R_{12} = 4\Omega$$

**Table 4-3: The two currents are not independent.**

$i_1$	$i_2$
0	0.026
0.4	0.021
0.8	0.016
1.2	0.011
1.6	0.005
2.0	0.000

<sup>7</sup> P.Horowitz, W.Hill, The art of electronics, 2<sup>nd</sup>Ed., (1995) p3,33

---

The value of  $R_{12}$  is assumed to stay constant in the calculations. However it increases as the current increases due to the higher temperature of the resistor. This increase is dependent on the resistivity coefficient of the column material. For the metal used here the resistance of the 1 meter column may increase with about  $1\Omega$  between  $i_1 = 0$  and  $i_1 = 2$  Amp as the temperature of the column ( $R_{12}$ ) increases from ambient to  $350^\circ\text{C}$ . Thus, the dependence of  $i_2$  on  $i_1$  may be slightly less than suggested by the preceding calculations.

This circuit possibly worked for the published results because very short column segments were used for temperature measurement. According to Phillips<sup>8</sup>, resistance of the column segment ( $R_{12}$ ) that is measured must be small relative to the resistor  $R_2$ . In our case  $R_{12} \approx 12\Omega$  and  $R_2 = 300\Omega$ . However, when shorter column segments are used, temperature-sensing resolution is sacrificed because the measured difference in resistance with a change in temperature is reduced.

Since the two currents are not independent, it is impossible to heat the column and measure the temperature simultaneously. This circuit may still be practical when pulse-width modulation is used for column heating. The measuring signal will then be applied during the off phases in between the heating pulses. Alternatively the circuit should work well when a separate sensing wire is used.

Additional problems encountered with this circuit were the 30mA required by the optical switch to operate properly while the counter chip on the board delivers only 5mA. The pulse train from the counter chip on the multifunction input/output board in the computer was however reasonably well maintained and only lost some of its sharpness on the rising edge of the pulse. This can in part also be attributed to the slow rise time of some of the capacitors and band pass filters required to clean up the noisy input signals. However, this did not interfere with measurements, which were always taken from the center of the high and low regions of each square wave.

---

<sup>8</sup> J.B.Phillips, Private communication.



#### 4.3.4 The current mirror circuit

Unfortunately it was not possible to get this circuit to function properly. The square wave was extracted from the DC signal through capacitor C2 (Figure 4-3), which formed part of a high band pass filter to decrease noise. The band pass filter, unfortunately, loads the signal and this decreases sensitivity. The *synchronized data acquisition* subprogram (LabVIEW program 4.3.4) reported a time-out error signal. This was probably due to the input signal being too small to trigger acquisition on the analogue to digital board. In an attempt to amend this problem, an additional operational amplifier was connected prior to the analog input into the computer. However, this distorted the square wave severely and measurement was impossible. Research attention at this point, out of desperation, was moved onto other temperature measurement possibilities. Since these were probably not fundamental problems with the circuit, an electronic engineer may in future solve the technicalities and allow this circuit to be used for resistive temperature measurement.

#### ***4.3.5 Resistance of heating element by Ohms' law***

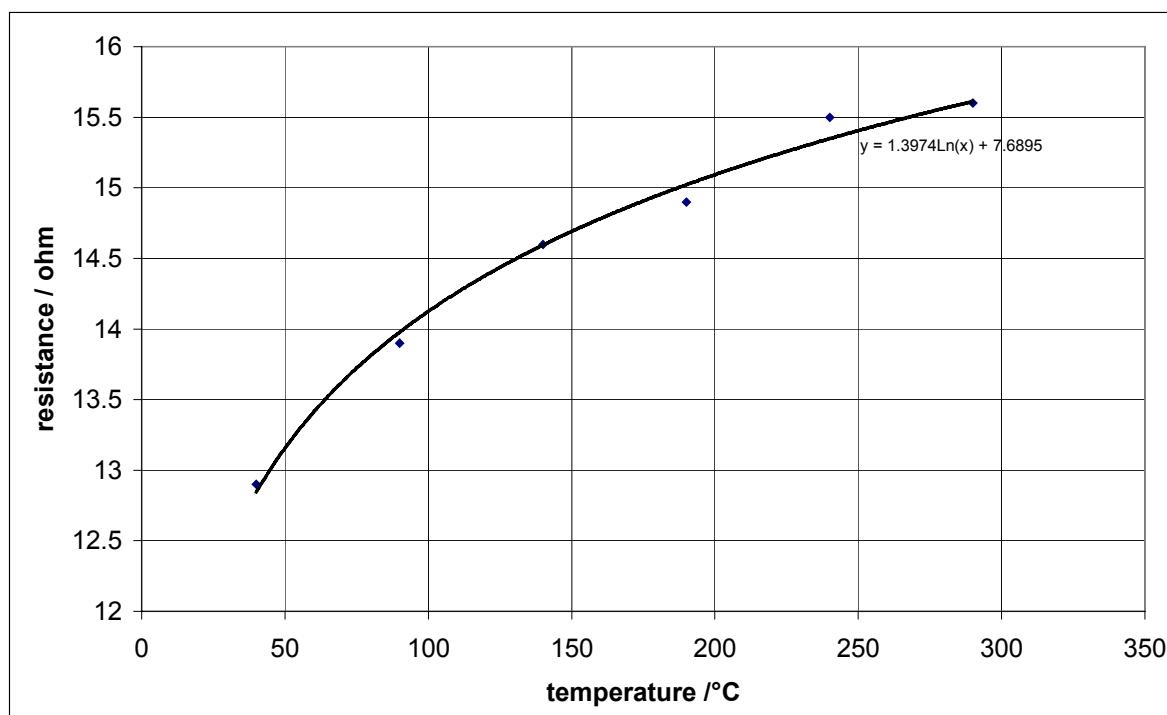
This is a far simpler approach to temperature measurement than the previous attempts. The resistance of the column is calculated from current and voltage drop measurements. The temperature is then calibrated against resistance.

The value of the current sensing resistor has a great influence on the sensitivity of the measurement. The larger the resistor, the larger the voltage measurement for an increase in current. However, larger resistors are more prone to self-heating. When a resistor heats up, its resistance changes and this will lead to erroneous readings as the resistance of the warm resistor is no longer known. The resistance of  $\approx 1\Omega$  obtained from using five  $4,7\Omega$  resistors in parallel is quite large for this type of application. However, internal heating was limited by using bulky resistors with a high wattage rating (25W each). The use of five resistors in parallel has the effect of dividing the current through each resistor by five, thus further reducing self-heating. The resistors were also mounted on a heat sink to aid effective dissipation of any produced heat.

Even when the column was not heated, a constant low current was still required for measurement purposes. It was found that at least 0.1A was needed for the circuit to operate satisfactorily. It is unlikely that 0.1A should cause significant heating of the column. When the temperature was increased by the host GC, a logarithmic relationship between resistance and temperature was obtained (Figure 4-8).

**Figure 4-8: Resistance calibrated against known temperatures.**

Maintained by the Host GC for the Resistance circuit. A measuring current of 0.1Amps was used.



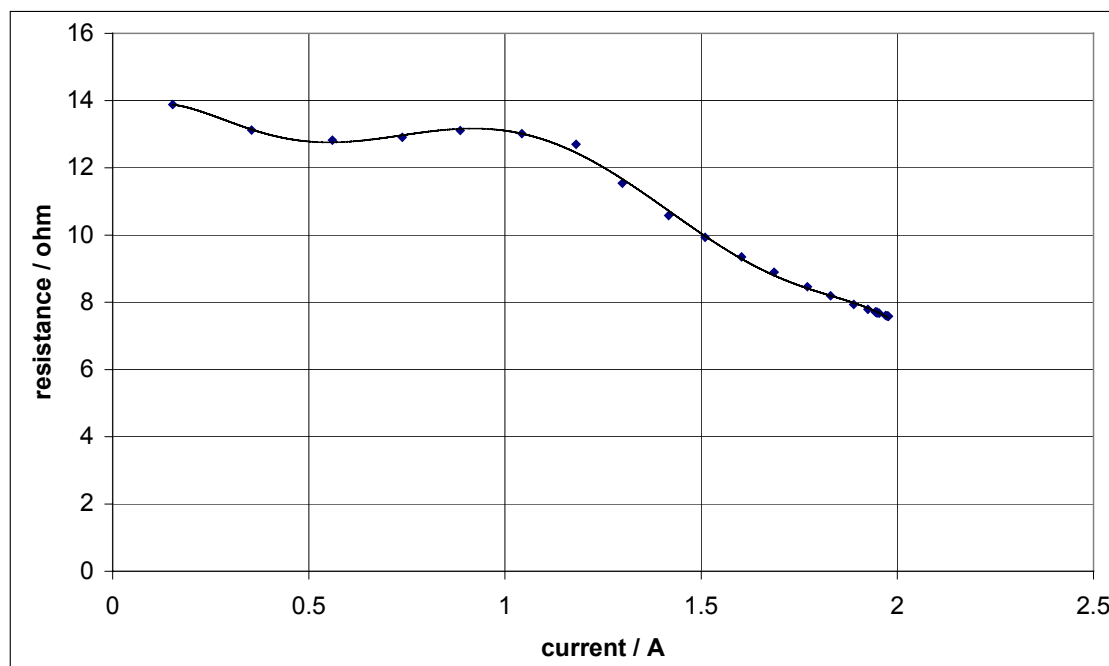
Noise was a bigger problem here than with the preceding circuits because two voltage readings were taken. One reading was taken for current calculation and the other for column voltage drop. This effectively doubled the noise on the resistance value which is calculated from both measurements.

Another problem encountered was that the analog input at the higher end of the column needed to face the full 30V of the heating current supply. Since this board and most general types of analog input boards have an input limit of  $\pm 10V$ , a three to four times voltage divider was required to avoid saturation of the amplifiers. 30 Volts were also uncomfortably close to the maximum allowable voltage (40V) on the

inputs, at which these boards are likely to be damaged. When voltage dividers were used on the inputs not only the offset was divided but also the small difference in voltage drop due to the increase in resistance with the concurrent increase in temperature. For a 1 meter column the resistance only increased by about  $1\Omega$  from 12 to  $13\Omega$  for the temperature range of 40 to  $250^{\circ}\text{C}$ . Thus, the use of voltage dividers significantly reduced the sensitivity of the measurements.

Unfortunately, when a heating current was applied and it was attempted to simultaneously calculate the resistance from the voltage and current measurements, very strange results were obtained: The slope stayed constant for the first 1A where after resistance appeared to decrease with an increase in current (Figure 4-9).

**Figure 4-9: Resistance appears to decrease with increased current.**



Despite numerous efforts to try and improve this result, which included using lower voltages across the column without voltage dividers, replacement of various components in the system, cleaning of the electrical contacts, etc, no solution has yet been found.

At this point further work with this circuit was postponed and the use of a micro-thermocouple described in the next section was investigated.

---

### 4.3.6 Thermocouples

#### 4.3.6.1 Thermocouple basics<sup>9</sup>

A thermocouple is a floating signal source and has an isolated ground reference point. This point is the connection between the two wires at the measurement point. The potential difference between the two legs of the thermocouple is produced due to differences in the Seebeck electromotive force (emf) produced along the lengths of the two dissimilar legs of the thermocouple. The Seebeck effect concerns the conversion of thermal energy into electrical energy. While the Seebeck emf can be referenced to 0 K, in practice the measured emf is often corrected by junction temperature compensation (CJC). CJC is an emf value that is produced at the known temperature of a reference junction. The SCB-68 connector accessory provides automatic CJC when used together with National Instruments E series boards by sacrificing one analog input. LabVIEW has built in reference tables that make the use of thermocouples extremely easy.

The use of thermocouples for temperature measurement on fast resistively heated capillary columns could be considered impractical. The major objection to the use of thermocouples is the additional thermal mass added to the spot where the thermocouple is connected. Increasing the thermal mass means that more electrical power is required to heat the zone. When constant power is supplied across the length of the column this zone may be colder than the rest of the column. A colder section has less resistance and will also heat at an even slower rate. The deciding factor in preventing a run-away situation under these conditions is how fast temperature can be equalized by conduction along the length of the column. Compounds can be trapped at this colder position in the column or peak tailing may result. Temperatures lower than the actual column temperature will be read by the thermocouple. However, to the best of our knowledge the use of thermocouples, directly on a GC column for temperature control, has not yet been reported on.

---

<sup>9</sup> R.M.Park, H.M.Hoersch, Manual on the use of thermocouples in temperature measurement, Philadelphia: ASTM manual series MNL 12, Chapter 1

#### 4.3.6.2 Very small thermocouples

Very small thermocouple wires have become commercially available. While these very small thermocouples can not currently be bought ready-made, we found an adequate success rate in preparing them in-house using the spot welding technique described in the Instrumentation Section 4.2.3.4. A well-prepared thermocouple has a diameter of only slightly more than 0.05mm. This is about the sum of the diameters of the two wires. The capillary column has a wall thickness of 0.25mm. This is significantly larger than the size of the micro-thermocouple.

#### 4.3.6.3 Peak profiles in comparison to a stirred air bath GC

Chromatograms were obtained with the Varian GC and by the resistive heating method at the maximum programming rate (50°C/min) obtainable with the Varian. Figure 4-11 and 4-12 show that earlier eluting peaks, up to hexadecane, display good retention-time correlation. Later eluting peaks, however, tend to exit the column much sooner with resistive heating than when the GC oven is used for heating. It has to be pointed out that the Varian doesn't follow the set ramp rate very well when the maximum rate is used, either<sup>10</sup>. This may result in an over-exaggeration of this anomaly.

**Figure 4-11: Chromatogram of C10-C24 n-alkane with thermocouple controlled temperature ramp. A 1 meter column programmed at 50°C/min; H2 at 1m/sec**

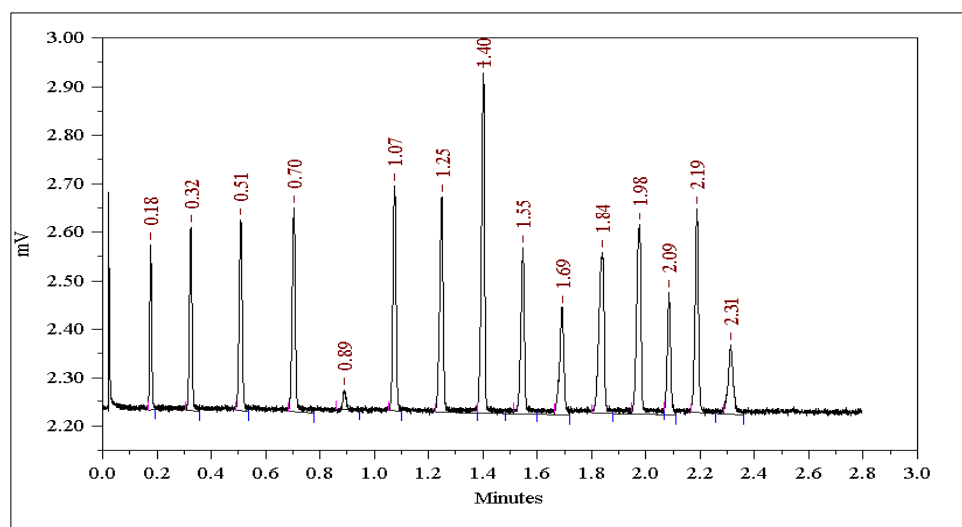
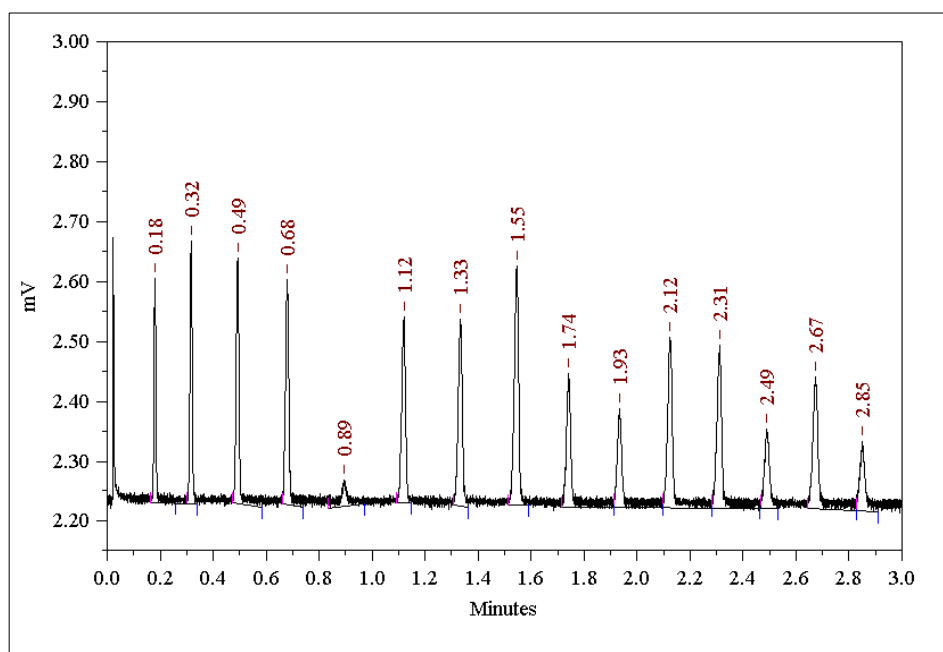


**Figure 4-12: Chromatogram of C10-C24 n-alkanes with the GC oven controlling the temperature ramp.** A 1meter column programmed at 50°C/min;



#### 4.3.6.4 Thermocouple placement

No peak distortion such as tailing is discernable from the chromatogram (Figure 4-11) and it is unlikely that a significant cold spot was formed by thermocouple placement. While the additional thermal mass was compensated for by heat conduction along the column, the measurement of the thermocouple did not accurately follow the capillary temperature at higher temperatures. The higher the temperature differential between the column and the environment, the faster heat is lost to the cooler surroundings. The thermocouple, just slightly removed from the column for insulation purposes, reads a lower temperature. Sending this apparent low temperature value to the feedback loop in the current-control program (LabVIEW program 3.a) called for an increase in the current output through the column. This caused the true temperature to increase to above the measured value and resulted in peaks of higher boiling n-alkanes to move progressively closer to each other.

Additional non-linear calibration will be required after installation to ensure accurate temperature measurements at high temperatures. Since this retention time effect was reproducible, at least within the same thermocouple installation, it is unlikely to cause major complications for most applications. However for each new installation the

measurement elution temperatures for later eluting compounds will be slightly different.

Placement of the thermocouple has a strong influence on temperature measurement accuracy and thus, retention times vary from placement to placement. It was difficult to ensure that the thermocouple was always attached with the same droplet size of glue and that it was placed with the same amount of glue between the thermocouple and the column i.e. that it was the same distance from the column. The thermocouple needs to be electrically isolated from the column to protect the analog inputs from the 30V present on the column. Thus the above results can still be improved on if the thermocouple can be placed even closer to the column.

**Figure 4-13: Two thermocouples placed and measured on the same column.**

Top line: Set point;  
Lower line: Thermocouple 1 (used for control);  
Bottom line: Thermocouple 2 (read-out only).

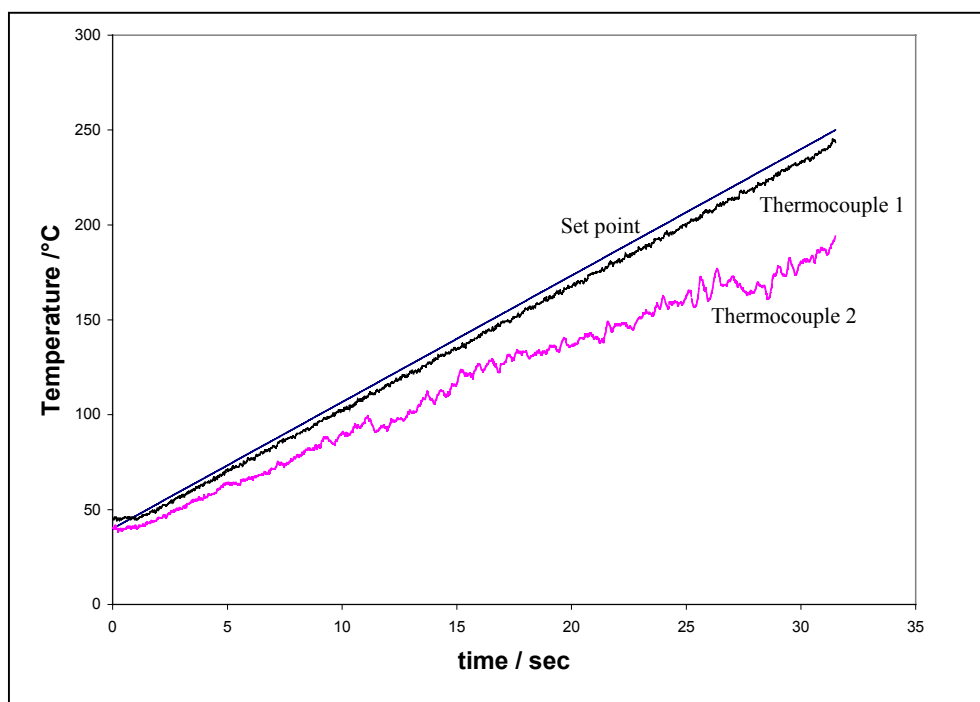


Figure 4-13 demonstrates the difference between two thermocouples placed and read simultaneously on the same column. Thermocouple 1 read a higher temperature than Thermocouple 2.

Note also the influence of the feedback control. Only the readings from Thermocouple 1 were used for feedback. This temperature appeared to follow the ramp with high

fidelity, as expected. Using a second, uncontrolled thermocouple illustrates that the temperature across the length of the column did not necessarily follow the ramp equally well. This creates the illusion of a smooth ramp profile because of the use of feedback on the thermocouple signal while the actual temperature may differ significantly from the set point. Some parts of the column may also have very different temperatures to the temperature at the point of measurement. Should thermocouple 2 have been used for temperature feedback control the reading of thermocouple 1 would have been above the set point and compounds would tend to elute earlier.

#### ***4.3.6.5 Stability problems***

After prolonged continuous use, the polyimide glue became brittle from repeated heating and cooling cycles. The thermocouple junction was also weakened, possibly due to differences in expansion coefficients of the two wires.

Due to the minute diameter of the wires they are extremely fragile and almost invisible to the human eye. Thus it has to be considered normal to replace the thermocouple after any kind of maintenance work inside the host GC oven by even the most careful worker.

#### ***4.3.7 Fixed function without feedback***

The control values from the computer during feedback controlled operation of many repeated ramps were recorded to obtain an average function. The coefficients had to be adjusted through an iterative process until the set ramp was followed with acceptable fidelity. This array of control values was sent to the current control circuit to obtain a temperature ramp that was applied to the column without feedback control.

#### ***4.3.8 Retention time reproducibility***

Reproducibility data have been published using many different units. When %RSD is used<sup>11</sup> the standard deviation (SD) is divided by the retention time. This means that

---

<sup>11</sup> E.U.Ermann, H.P.Dharmasena, K.Carney, E.B.Overton, J.Chrom Sci. 34 (1996) p533



later eluting peaks appear to be more reproducible than earlier ones even when they are not in absolute terms.

Some authors provide reproducibility data as SD divided by the peak width<sup>12</sup>. While the peak width defines what level of reproducibility is acceptable, other factors, not directly linked to reproducibility, are brought into account. This makes direct comparison between instruments with different column performances difficult, as poor retention time reproducibility may be obscured by poor column performance. It is the opinion of the author that the use of standard deviation should be encouraged as a primary means of reporting retention time reproducibility, as it is the unit least likely to obscure the facts and can be converted into any of the other units if additional information such as retention times and peak widths are provided.

Short term, run to run, reproducibility using the thermocouple is good and compares favorably with commercial instrumentation. Table 3 demonstrates that retention time reproducibility produced by the thermocouple system was about 2 to 4 times worse than for commercial instrumentation. However it was at least twice as good as other in-house manufactured, resistively heated GC instrumentation.

The influences of various factors on the retention time stability were investigated. Electronic noise originating from the six-port valve was measured on the thermocouple input with an oscilloscope. However, it did not have a significant influence on reproducibility, whether the valve was on or off. When a 20Hz low band pass filter was used instead of the 40Hz filter, used for the results obtained in Table 3-4, the average SD increased to 0.134. Changing the gain on the PID controller improved the SD for earlier eluting compounds, however, the average increased to 0.127.

Slightly better retention time reproducibility was obtained when a pre-defined function was used for the current ramp without feedback control. However, this approach is very inflexible because a new function had to be generated for each new combination of starting temperature and ramp rate. Great care needed to be taken to ensure that the conditions where the ramp was defined, exactly matched the

---

<sup>12</sup> J.Dalluge, R.Ou-Aissa, J.J.Vreuls, U.A.Th.Brinkman, HRC 22 (1999) p459

conditions when the ramp was applied. Any disturbance during the ramp produced unpredictable results. When a function without feedback was used to produce an SFCxGC<sub>fp</sub> run, results were very poor. This was probably due to the difficulty in fixing the cryogenic starting temperature.

**Table 4-4: Standard deviation of retention times in seconds**

Alkane	Thermocouple Method 4	Function-no feedback Method 5	Collinear <sup>11</sup> at-column heater	EZ-Flash <sup>12</sup> 200°C/min	EZ-Flash 300°C/min
9				0.052	
10	0.073	0.078	0.57		
11	0.072	0.062	0.37		
12	0.080	0.049	0.42		0.075
13	0.072	0.041	0.39	0.048	
14	0.068	0.044	0.42		
15	0.071	0.045	0.28		
16	0.087	0.051	0.36		
17	0.107	0.052	0.27	0.052	
18	0.123	0.057	0.50		
19	0.129	0.071	0.45		
20	0.141	0.079	0.52		
21	0.143	0.087		0.040	
22	0.127	0.096			
23	0.105	0.107			
24	0.097	0.110			
26				0.040	
<b>average</b>	<b>0.099</b>	<b>0.069</b>	<b>0.42</b>	<b>0.046</b>	<b>0.075</b>

#### 4.3.9 Optimization of ramp rate

Blumberg<sup>1</sup> suggested that an optimum ramp rate exists where an adequate separation of a required number of analytes can be attained in the shortest time. Furthermore, the temperature programming rate is a translatable quality and can be expressed as a rate

normalized to dead time. Thus, it is relatable to the carrier gas flow rate through the column. Finding the optimum separation conditions entails changing the carrier gas flow and temperature programming rate in a concerted fashion so as to maintain a constant normalized ramp rate. This requires calculation of the ramp rate for each new dead time obtained at the set flow rate. The aim is to maximize the peak capacity for a given column in the shortest available time.

Peak capacity was measured while maintaining the temperature-programming rate at  $10^{\circ}\text{C}/\text{tm}$ . Both flow rate and temperature-programming rate was changed for each data point. The values are reported in Table 4-5:

**Table 4-5: Ramp, flow rates and peak capacity for  $\text{H}_2$  at  $10^{\circ}\text{C}/\text{tm}$**

Programming rate ( $^{\circ}\text{C}/\text{min}$ )	Linear flow rate ( $\text{cm}/\text{s}$ )	Total analysis time (min)	Peak capacity
110	25	1.85	59
230	50	0.90	62
330	72	0.61	60
430	93	0.47	56
530	115	0.41	53
650	140	0.32	48
760	165	0.29	44
900	195	0.22	38

Hydrogen carrier gas at  $10^{\circ}\text{C}/\text{t}_m$  demonstrates that the maximum in peak capacity can already be obtained at a total analysis time of 0.6 minutes. After this point it a plateau is reached. Figure 4-14 also emphasizes the need to exchange  $\text{CO}_2$  for  $\text{H}_2$  as mobile phase for fast GC in the  $\text{SFC}\times\text{GC}_{\text{ftp}}$ .  $\text{CO}_2$  only approached the maximum peak capacity obtained by  $\text{H}_2$  of  $n_c \approx 60$  after more than twice the analysis time. This is to be expected, due to the associated higher resistance to mass transfer in the mobile phase. This can further be explained as a larger C-term in the Van Deemter equation context.

---

Note that the peak capacity was only calculated as the sum of peak capacities between decane and tetracosane. For the true peak capacity these values have to be extrapolated to include the separation space between decane and an unretained compound, adding approximately 12 peaks to provide a total of  $n_c = 72$  in thirty seconds.

Most excitingly, the graph allows for the simultaneous optimization of program and flow rate, all in one.

Blumberg suggested  $10^\circ\text{C}/\text{tm}$  as default for most applications. However a higher value of  $18^\circ\text{C}/\text{tm}$  was indicated for low pressure drop conditions. The typical inlet pressures of between 1.1 and 1.4 atm, used with the 1-meter column, pertained to the low pressure drop region. Thus  $18^\circ\text{C}/\text{tm}$  was also investigated. For  $\text{H}_2$  it appears as if the maximum peak capacity obtainable was slightly lower at  $18^\circ\text{C}/\text{tm}$  than at  $10^\circ\text{C}/\text{tm}$ . However, the performance normalized to analysis time ( $n_c/t_a$ ) was higher. This correlates well with the published results<sup>1</sup>. For both  $\text{H}_2$  and  $\text{CO}_2$  a marginal increase, less than 10%, was observed on the faster side of the trend line. This indicates that the optimum ramp rate is probably situated on a plateau.

The normalized ramp rate of  $450^\circ\text{C}$  and a flow rate of  $100\text{cm}/\text{s}$  were found to be optimal. These conditions were used for the chromatogram depicted in Figure 4-15. It corresponds to a normalized ramp rate of  $10^\circ\text{C}/\text{tm}$  and a peak capacity of  $n = 72$ . A ramp rate of  $18^\circ\text{C}/\text{tm}$  requires faster actual ramp rates with a consequent decrease in reproducibility and ramp tracking fidelity (with present instrumentation), but without realizing a substantial increase in peak capacity at very short analysis times. Hydrogen carrier gas at  $10^\circ\text{C}/\text{tm}$  demonstrated the maximum in peak capacity (or minimum in peak height) obtained at a total analysis time of 0.6 minutes. After this point, a logarithmic relation was no longer followed but a plateau was reached. This is the result of increasing peak widths due to longitudinal diffusion (B-term of the Van Deemter equation).

**Figure 4-14: Peak capacity maximization by simultaneous optimization of flow and temperature programming rate.**

■ CO<sub>2</sub> at 10°C/tm, ◆ H<sub>2</sub> at 10°C/tm, × CO<sub>2</sub> at 18°C/tm, ▲ H<sub>2</sub> at 18°C/tm.

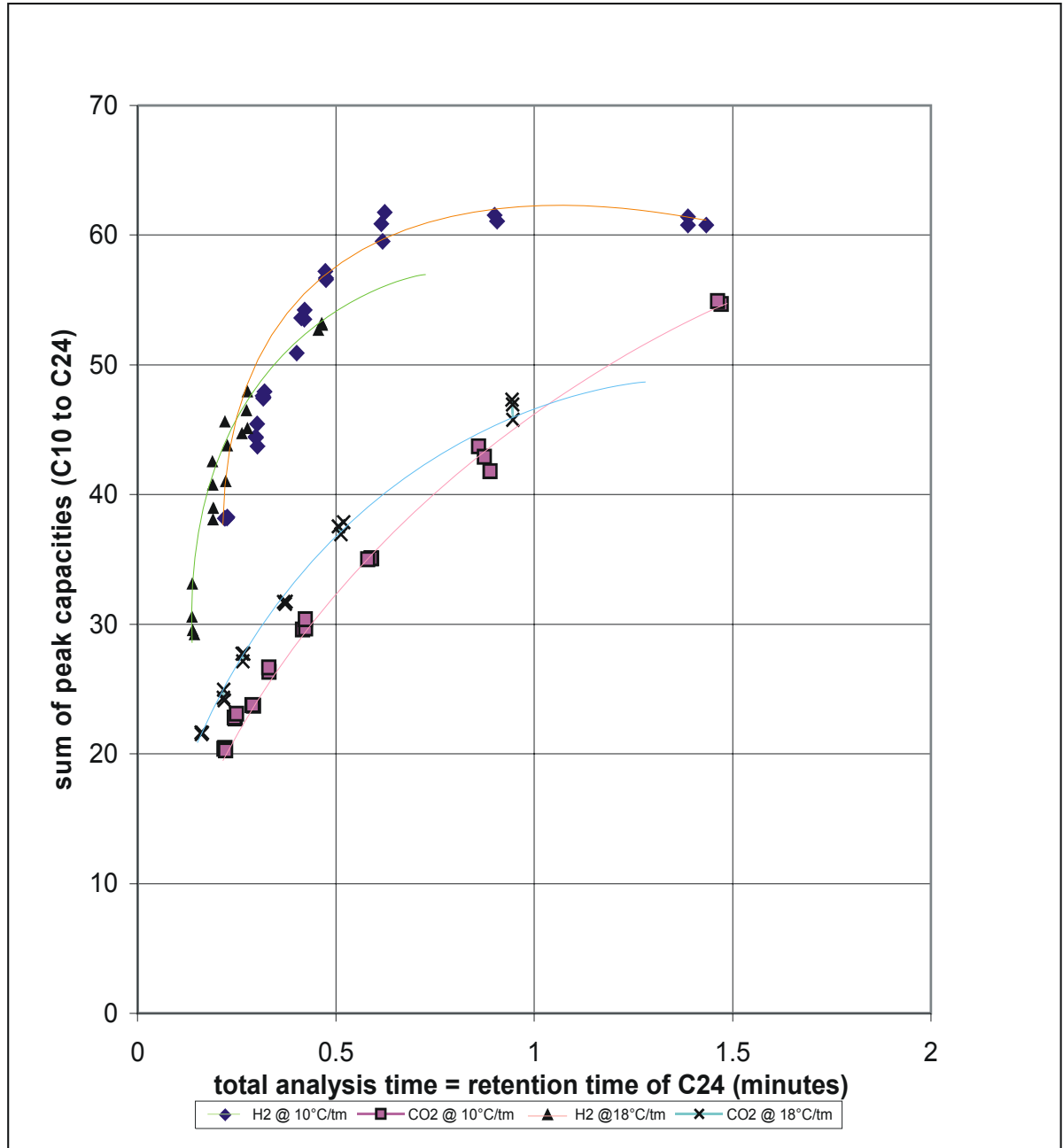
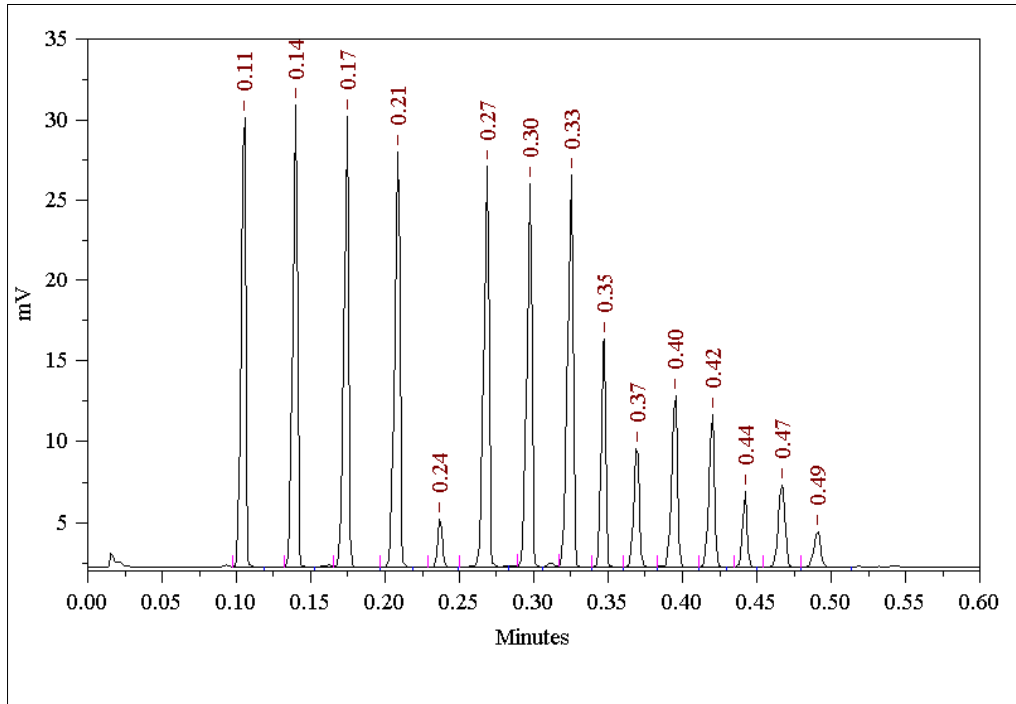


**Figure 4-15: A typical chromatogram of n-alkanes of C10 to C24 at optimum conditions: 50°C to 300°C at 450°C/min and flow rate of 100cm/sec.**



---

## 4.4. Conclusions

Measurement of the temperature through column resistance while simultaneously heating the column by continuously supplying current produced many problems: The measurement signal was small in comparison to the DC-heating current. This DC offset saturated the operational amplifiers on our analog to digital converter board. The sensing voltage could be electronically extracted from the DC heating current as an AC measurement signal. Alternatively, a voltage divider could be used to bring the measured signal back into the acceptable range of the amplifier. However, with a voltage divider, the sensing voltage was divided together with the offset voltage and this led to a loss in accuracy of temperature measurement.

These problems will disappear if pulse width modulation is used. Ermann et.al. , as well as the commercial Flash-GC instrument, uses PWM for temperature control. During the less noisy moment when the DC-current used for heating is momentarily switched off, the temperature can be more accurately measured. However, pulse width modulation requires faster acting electronics, as the heating modulation needs to be quite fast to ensure smooth ramp profiles.

Compared to the technical problems encountered with the other temperature measurement circuits, use of the thermocouple allowed for simpler temperature control. The lack of mechanical stability of micro thermocouples following repeated heating and cooling cycles and the general fragility of these wires were the greatest disadvantage.

Use of a commercial stainless steel column simplified the design and reduced GC cycle times due to faster cooling.

Results obtained with thermocouples compared reasonably to chromatograms obtained with conventional GC instrumentation. Retention time reproducibility also compared well with other resistively heated GC instrumentation. On average standard deviation of  $SD=0.099$  seconds were obtained. It is still however, difficult to distinguish between a single peak and two closely eluting peaks in the 3D

chromatogram. (See Chapter 9). Thus ways to improve on retention stability should be sought.

The stability of thermocouples following repeated heating and cooling cycles and the general fragility of these microscopic wires, however, demand a more robust temperature measurement approach.

Ways should be found to measure the temperature independently from the heating circuit. To this end, either pulse width modulation or a separate sensing wire is suggested.

The use of a separate heating sleeve should be considered, as this will provide increased flexibility in the choice of stationary phases and columns dimensions. This will also facilitate the use of a separate sensing wire.

At a normalized heating rate of  $10^{\circ}\text{C}/\text{tm}$  the maximum peak capacity of  $n=72$  was obtained at a programming rate of  $450^{\circ}\text{C}/\text{min}$  and a linear flow rate of  $100\text{cm}/\text{sec}$ . The maximum peak capacity decreased when a normalized programming rate of  $18^{\circ}\text{C}/\text{tm}$  was used while the normalized performance increased.

Using  $\text{H}_2$  as opposed to  $\text{CO}_2$  the same separation number (55) could be achieved in one third of the analysis time (1.5 minutes versus 0.5 minutes), experimentally verifying the expected advantage of replacing  $\text{CO}_2$  with  $\text{H}_2$  in our SFCxGC interface. Alternatively, for 0.5 minutes hydrogen carrier gas provides almost twice as much separation number as  $\text{CO}_2$  (60 versus 33).

Peak capacity versus analysis time curves at normalized temperature programming rates have apparently not been reported before and are a great tool in the practical optimization of fast temperature programmed GC.